ACS OMEGA

Article

Cite This: ACS Omega 2019, 4, 19818−19828

http://pubs.acs.org/journal/acsodf

Catalytic Palladium-Based and Iron-Based Membrane Reactors: Novel Strategies of Synthesis

Verónica Pinos-Vélez,[†,‡] Carla di Luca,[†,§] Dana G. Crivoi,[†,∥,⊥] Francisco Medina,[†,∥] and Anton Dafinov*[,†,∥]

[†]Departament d'Enginyeria Química, Universitat Rovira i Virgili, Av. Països Catalans, 26, Campus Sescelades, Tarragona 43007, Tarragona, Spain

[‡]Departamento de Recursos Hídricos y Ciencias Ambientales, Facultad de Ciencias Químicas, Universidad de Cuenca, Av. 12 de abril y ciudadela universitaria, Cuenca 010107, Azuay, Ecuador

[§]Departamento de Ingeniería Química-Facultad de Ingeniería, Universidad Nacional de Mar del Plata e Instituto de Ciencia y Tecnología de Materiales (INTEMA-CONICET), Av. J. B. Justo 4302 (B7608FDQ), Mar del Plata 7600, Buenos Aires, Argentina

[∥]EMaS-Research Center on Engineering of Materials and Micro/NanoSystems Rovira I Virgili University Marcel-li Domingo, Tarragona 43007, Tarragona, Spain

[⊥]Chemistry Research Laboratory, University of Oxford, 12 Mansfield Road, Oxford OX1 3TA, Oxfordshire, U.K.

Supporting Information

ABSTRACT: Several procedures were employed in the preparation of different Pd- and Fe-based catalytic membrane reactors (CMRs) via the normal wet impregnation method, reverse filtration of a microemulsion, sputtering method, and the precipitation of a Fe complex. Depending on the chosen procedure, the metal active phase can be found on the exterior and/or interior part of the CMR or even in its pores in concentrations between 0.05 and 2 wt %. Moreover, we have managed to implement a unique systematic process to grow hydrotalcite in the pores of a Pd-CMR. To exemplify the activity of these new CMRs, we have tested them in the peroxidation of phenol and in situ epoxidation of *trans*-chalcone.

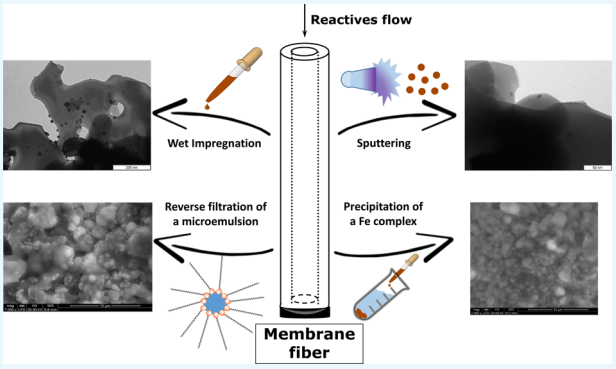

1. INTRODUCTION

Over decades, chemistry and chemical engineering have been developed and optimized to assure the best time-space yield. From the plethora of chemical transformations, gas/liquid reactions have been intensively studied, not only because they present an efficient atom economy but also because they are environmental-friendly processes.[1] However, the use of a solid catalyst in these reactions will create a three-phase system, posing a series of challenges for the reactor designing, such as the contact between the three phases and the flow boundaries.[2] One way to overpass these limitations and improve the interphase contact is to use a catalytic membrane reactor (CMR), defined as a device combining a membrane-based separation and a chemical reaction in one unit.[3] The most representative features of CMRs are their selective removal of a product, retention of the solid phase (such as a solid catalyst), distribution of a reactant, and catalyst support.[4]

In general, a CMR contains either a polymeric membrane or an inorganic one, but the latter is preferred because of its thermal stability, chemical resistance, and mechanical strength.[5] Besides the constituent material, the porosity of the membrane is critical for its potential catalytic applications, as the permselectivity increases with the pore size.[6] Moreover, the open pore path and transmembrane pressures are essential in providing an easier access of the reactants to the active sites.[7]

In terms of the catalytic active centers, the CMRs can be divided into two classes: one in which the membrane is the catalyst in the reaction (e.g., zeolites or dense metallic ones) and the other where the membrane is inert and the catalyst is incorporated through different means: physical or chemical vapor deposition, ion exchange, sol−gel, or impregnation.[8] CMRs may include conductive or chemically active materials, which may operate with external stimuli such as light, electrical current, chemical activation, enzymatic response, or their combination.[9] No matter how the catalyst is loaded, one CMR can have multiple uses: as an extractor, as a distributor, and/or as a contactor; in the latter one, the reactants are separately introduced from each side of the membrane and they meet in the region where the catalyst is found.[10] There are many

Received: August 21, 2019
Accepted: November 5, 2019
Published: November 14, 2019

DOI: 10.1021/acsomega.9b02706
ACS Omega 2019, 4, 19818−19828

aspects that must be taken into consideration when the contactor catalytic membrane is chosen to perform any reaction. These aspects are catalyst stability on the membranes, size or shape of catalyst particles, distribution of the catalyst along the membrane surface, and the stability of the catalyst under reaction conditions, as well as the ability of the catalyst to regeneration.[11]

On this basis, CMRs have been extensively used in numerous reactions, such as the production of H_2O_2 from H_2 and O_2[7,12−15] or from H_2 and airborne oxygen under very mild conditions,[12] nitrate ion reduction using H_2 generated in situ from formic acid[6] and hydrogenation,[7,16−20] or oxidation of different organic compounds.[18,20−22] The CMR technology presents a huge potential for different applications as it reduces the investment costs, increases the energy efficiency, and can be employed for a wide range of conditions with the aim of increasing the conversion in equilibrium limited reactions.[23] Although there is a growing interest in the membrane reactor technology,[24] the attention is focused more on the catalytic applications and less on the preparative methods.

In this context, we report a series of novel preparative methodologies to create palladium- and iron-based corundum membrane reactors, shifting the CMRs toward a new horizon: hybrid-CMR containing not one but two different catalytic entities. Palladium and iron were chosen as the main active metals as Pd is known to be the key catalyst in hydrogen peroxide synthesis, while Fe offers significant advantages compared to precious metals, as it is an abundant metal in the earth crust and its compounds are relatively nontoxic.[25] To validate the importance of these new CMRs, we tested their activity in reactions with potential industrial applications: peroxidation of phenol (an organic pollutant)[26] and in situ epoxidation of *trans*-chalcone (an example of an α,β-unsaturated ketone).[27]

2. RESULTS AND DISCUSSION

For a clear comparison between all the CMRs prepared using different methods, Table 1 presents the active phase contents.

Table 1. Summary of the Active Phase Contents for the Different Pd- and Fe-Based CMR

entry	CMR	method	pore size (nm)	% wt active phase
1	Pd-CMR_s	sputtering	1400	0.06 Pd
2	PdCu-CMR_m	microemulsion	1400	0.3 Pd, 0.8 Cu
3	HT-Pd-CMR_i_a	impregnation	1400	0.75 Pd, 0 HT
4	HT-Pd-CMR_i_b	impregnation	1400	0.75 Pd, 2 HT
5	Fe-CMR_i	impregnation	20	2.1 Fe
6	Fe-CMR_p	precipitation of Fe complex	20	0.05 Fe
7	Fe-CMR_m	microemulsion	20	0.3 Fe

In terms of active phase distribution, the CMRs prepared by impregnation displayed the presence of the active phase (Pd or Fe) throughout the entire section of the hollow fiber (Figure 1a), while those prepared by sputtering, precipitation, and microemulsion presented a preferential distribution of the active species on the external surface of the CMRs (Figure 1b). This feature can be advantageous to avoid high consumption of reactants (deposited metallic species and parasitic

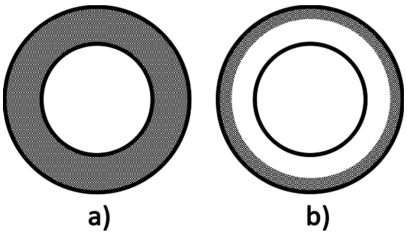

Figure 1. Catalyst distribution for the CMR hollow fibers prepared by (a) impregnation and (b) microemulsion, precipitation, and sputtering.

reactions), favoring the contact at the external surface of the CMRs. We have already shown[28] that Pd is selectively deposited over the external surface of the membrane.

2.1. Palladium-Based CMR. *2.1.1. Characterization.* In order to examine the Pd and PdCu particles on the CMRs, pieces of reactors were ground into fine powder and dispersed in ethanol. Figure 2 presents the picture of the original

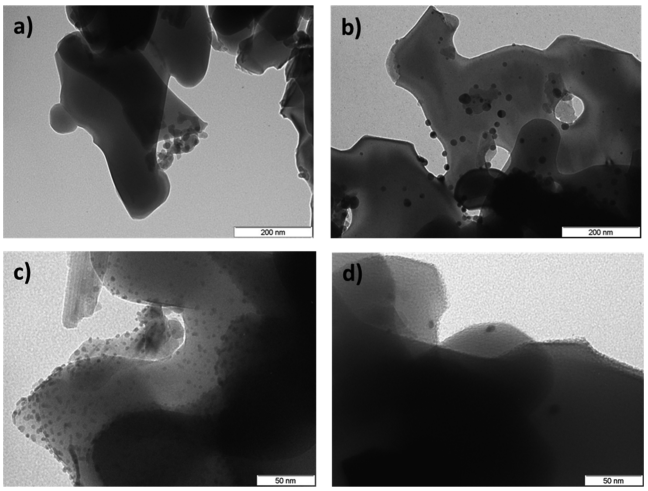

Figure 2. TEM images of the ground powder of the (a) initial corundum CMR, (b) Pd-CMR_i obtained by impregnation, (c) PdCu-CMR_m obtained by microemulsion, and (d) Pd-CMR_s obtained by sputtering.

corundum reactor, the Pd-CMR prepared by impregnation (further used to grow HT), the PdCu-CMR prepared by microemulsion (PdCu-CMR_m), and Pd-CMR prepared by sputtering (Pd-CMR_s):

The ground corundum, unmodified, presented bulky, nonuniform parts, as can be seen in Figure 2a. The Pd-CMR_i obtained by impregnation using a $PdCl_2$ solution presented Pd nanoparticles (NPs) with an average size of 16.5 nm (Figure 2b). On the contrary, by employing the reverse filtration of a microemulsion, we managed to uniformly distribute PdCu NPs over the entire surface of the CMR, obtaining a smaller NP average size of ca. 3.8 nm (Figure 2c). Last but not the least, the Pd-CMR_s prepared by sputtering presented an average size of the NPs of 4.5 nm (Figure 2d).

Crystallinity, composition, and the distribution of the catalytic phases of the Pd-CMR were analyzed at different selected areas of the hollow fiber by μ-XRD. Figure S1 in the Supporting Information presents the diffractogram of the initial tubular hollow fiber (Φ: 1400 nm); as can be observed, the fresh membrane exhibited typical peaks of α-Al_2O_3 (JCPDS

DOI: 10.1021/acsomega.9b02706
ACS Omega 2019, 4, 19818−19828

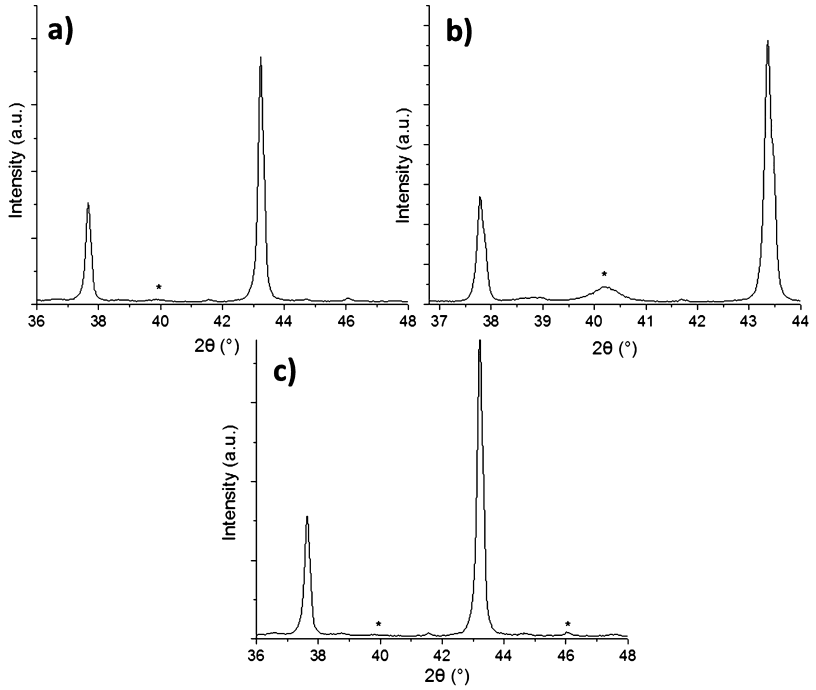

Figure 3. μ-XRD of Pd-based CMRs: (a) Pd-CMR_s; (b) Pd-CMR_i; and (c) PdCu-CMR_m; * highlights the peak positions corresponding to the Pd metal.

00-046-1212). Using the same procedure, we have analyzed the different Pd-CMRs. Along with the peaks corresponding to the corundum phase (observed at the 2θ angles 37.78 and 43.36°), we detected the presence of a new peak corresponding to the active phase (Pd) for the Pd-CMR_i (Figure 3b) and PdCu-CMR_m (Figure 3c). As expected, no visible peak was detected in the diffractogram of the Pd-CMR_s (Figure 3a), as the Pd loading was very low (entry 1, Table 1).

To prepare the hybrid HT-Pd-CMR, we decided to use the Pd-CMR prepared by impregnation as it contains the highest amount of Pd and presented the highest activity in the hydrogen peroxide synthesis. Our first try was based on immersing the 0.75 wt % Pd-CMR into a water suspension of HT, defined as Method A. Upon applying the vacuum, the HT was unevenly distributed over the external surface of the CMR, and after the drying and calcination processes, the entire HT was completely lost. This suggests that the HT was not able to penetrate the pores of the membrane. The X-ray diffraction (XRD) diffractogram of the CMR did not show the presence of the HT neither in the interior nor in the exterior of the membrane reactor.

The second method used (Method B) proved to be more efficient. When the 0.75 wt % Pd-CMR previously immersed in the Mg and Al salt solutions was submerged in the 2 M NaOH solution, the HT crystals started to grow in the pores of the reactor, a phenomenon observed with the naked eye. After in-depth washing, drying, calcination, and reduction steps, the HT crystals still remained in the CMR pores as observed from the XRD diffractogram of a small portion of the CMR (Figure 4).

2.1.2. Catalytic Results Using the Pd-CMR. The use of a CMR presents several advantages over the conventional powder catalyst, the most important one being the improvement of the three-phase contact. The use of CMR in the direct H_2O_2 synthesis requires a membrane intrinsically active for catalytic reactions, for example, dense metal (e.g., Pd), zeolites,

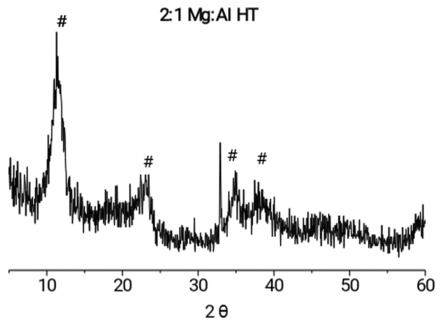

Figure 4. XRD from a sample of the HT-Pd-CMR_b (where # stands for the characteristic diffraction peaks of the Mg−Al hydrotalcite).

or inert membranes with an incorporated catalytic active phase.[29] Over time, the CMRs have become the benchmark of the direct hydrogen peroxide synthesis because of their great advantages over the conventional catalysts, which are as follows: (i) the distribution of the gases avoids the explosion mixture; (ii) the active phase can be easily regenerated, and (iii) there is a lower deactivation of the catalysts.[8]

A variety of procedures were implied to improve the performance of the CMRs for the direct synthesis of hydrogen peroxide[12−14,30−35] culminating with the work of Osegueda et al. who used a commercial hollow fiber impregnated with palladium.[15,28] This CMR was used for the production of H_2O_2 in contaminated wastewater effluents, and it was observed that the hydrogen peroxide obtained in the pores of the CMR is further transformed into the hydroxyl radicals, which oxidize the undesired organic compounds.

Epoxides are versatile intermediates in the production of complex molecules used in medicine, perfumery, and so forth. Based on our experience in using CMR for the production of hydrogen peroxide directly from hydrogen and oxygen, we have focused our attention in the in situ epoxidation of *trans*-chalcone. This reaction requires the hydroperoxide anions

DOI: 10.1021/acsomega.9b02706
ACS Omega 2019, 4, 19818−19828

Table 2. Screening of Solvents for the in Situ Epoxidation of *trans*-Chalcone Using the Hybrid HT-Pd-CMR_i_b

Entry[a]	Solvent	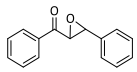 Selectivity (%)[b]	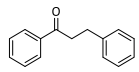 Selectivity (%)[b]	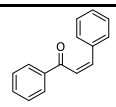 Selectivity (%)[b]	Conversion (%)[b]
1	H_2O / MeOH	6	65	29	40
2	MeOH	9	45	46	26
3	EtOH	0	22	78	21
4	2-Propanol	0	60	40	46
5	DMSO	0	100	0	100
6	ACN	0	55	45	32
7	Heptane	0	61	39	33

[a]Typical procedure: HT-Pd-CMR_i_b closed to one end and passing 30 N mL/min of H_2 to the other end was introduced in 40 mL of the solvent containing 10 mg of *trans*-chalcone; oxygen was directly bubbled in the mixture. After 6 h, the solvent was evaporated. [b]Determined from ^{1}H NMR spectra.

Table 3. Influence of Temperature on the in Situ Epoxidation of *trans*-Chalcone

Entry[a]	Temperature	Solvent	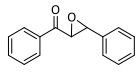 Selectivity (%)[b]	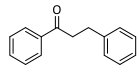 Selectivity (%)[b]	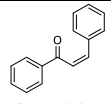 Selectivity (%)[b]	Conversion (%)[b]
1	r. t.	MeOH	9	45	46	26
2	0 °C	MeOH	19	30	51	43
3[c]	r. t	MeOH	22	23	55	29

[a]Typical procedure: HT-Pd-CMR_i_b closed to one end and passing 30 N mL/min of H_2 to the other end was introduced in 40 mL of methanol containing 10 mg of *trans*-chalcone; oxygen was directly bubbled in the mixture. After 6 h, the solvent was evaporated. [b]Determined from ^{1}H NMR spectra. [c]Extra H_2O_2 was added.

rather than the hydroxyl radicals; hence, the presence of a base in the reaction medium is of crucial importance;[36,37] thus, creating a hybrid CMR containing Pd and a basic catalyst, such as a hydrotalcite, seems to be a viable alternative.

The hybrid CMR prepared by Method B (HT-Pd-CMR_i_b) was used in the in situ *trans*-chalcone epoxidation using a series of solvents both protic and aprotic, as can be shown in Table 2. The hydrogenated product (Figure S2 in the Supporting Information) was obtained in all of the cases along with the *cis*-chalcone, but the epoxide was observed only when methanol was used as the solvent (entries 1 and 2, Table 2). Its formation was confirmed from ^{1}H NMR, as can be seen in Figure S3 in the Supporting Information. Although the epoxide could not be isolated in the other tested solvents, the presence of the *cis*-chalcone is a clear proof that the hybrid CMR is active in the in situ epoxidation of chalcone, as will be explained further in this study.

As gas solubility is temperature-dependent, we have studied the in situ epoxidation of *trans*-chalcone using the HT-Pd-CMR_i_b at 0 °C. As expected, in these conditions, the solubility of oxygen in methanol increased considerably, leading to a higher production of hydrogen peroxide and a decrease in the hydrogenation process (entry 2, Table 3). One can deduce that the limiting factor in the epoxidation reaction is the production of hydrogen peroxide, which also hinders the undesired reaction. To test this hypothesis, we have rerun the reaction in MeOH at room temperature but added an additional hydrogen peroxide (entry 3, Table 3). Not only that the selectivity of the hydrogenated product decreased, but an increase in both the epoxide and the *cis*-chalcone was observed.

As mentioned above, the hydrogen flow is subjected through one end of the CMR, while the other end is kept closed, creating a pressure difference, which forces the hydrogen molecules to exit through the CMR pores. The pores, containing Pd particles, will activate the hydrogen, which, in the presence of an oxygen molecule, will form hydrogen peroxide. Depending on the environment, the newly formed H_2O_2 can either decompose to water or transform into hydroxyl radicals.

In the case of the HT-CMR, the pores contained both HT and Pd; thus, the formation of the hydrogen peroxide will subsequently be transformed into the hydroperoxide anion as can be seen in Scheme 1A. The hydroperoxide anion and a *trans*-chalcone molecule (**1a**) assemble in a complex to form the corresponding peroxide enolate intermediate (**2**). This intermediate is not stable, and will eliminate a hydroxide to give the corresponding epoxide (**3**). Isotope-labelled studies of the normal Weitz−Scheffer oxidation of *trans*-chalcone have shown that the enolate (**2**) can easily undergo rotation, leading to the formation of *cis*-chalcone.[38] The formation of the epoxide (**3**) is strongly related to the orientation of the O−O bond in respect to the π system: the O−O bond has to be antiperiplanar to enable an overlap with the O−O antibonding orbital. In other words, because of the steric hindrance and the bulky environment, the *cis*-chalcone-enolate is unable to favor the epoxide production, thus leading to the formation of *cis*-chalcone (**6**).

On the other hand, the presence of activated hydrogen on the surface of Pd favors the hydrogenation reaction. The mechanism of this reaction is not exactly known, but, besides the hydrogen molecules already bonded, *trans*-chalcone has the

DOI: 10.1021/acsomega.9b02706
ACS Omega 2019, 4, 19818−19828

Scheme 1. Proposed Mechanism for the in Situ Epoxidation of *trans*-Chalcone and Hydrogenation of *trans*-Chalcone Using HT-Pd-CMR_i_b: (A) Epoxidation Reaction; (B) Hydrogenation Reaction

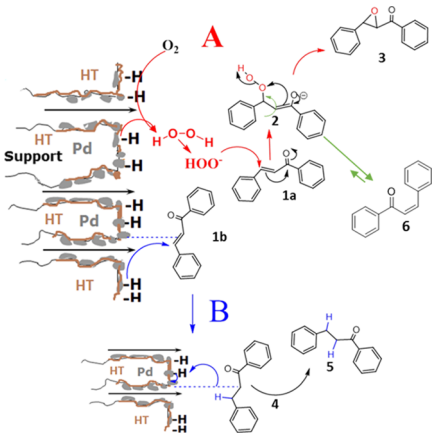

ability to bind to the surface/pores of the CMR (Scheme 1B); palladium activates the π bond system of the *trans*-chalcone double bond (**1b**) and the molecule is not removed from the surface until the transfer of a hydrogen atom is not completed (**4**).

2.2. Iron-Based CMR. Similar to Pd-CMR, we have analyzed Fe-doped CMR using different analytical techniques in order to assess (i) the size and shape of the hematite NPs synthetized by a w/o microemulsion method [transmission electron microscopy (TEM)]; (ii) surface characteristics of the synthetized CMR and Fe distribution in different areas of the reactors [environmental scanning electron microscopy (ESEM)−energy-dispersive X-ray (EDX)], and (iii) the crystallinity and dispersion level of loaded iron species (μ-XRD). A detailed description of these techniques is provided in the Supporting Information.

2.2.1. Characterization. The hematite NPs synthetized by the w/o microemulsion method described in Section 4.1.2.3 were analyzed by TEM (Figure 5). As can be observed, the

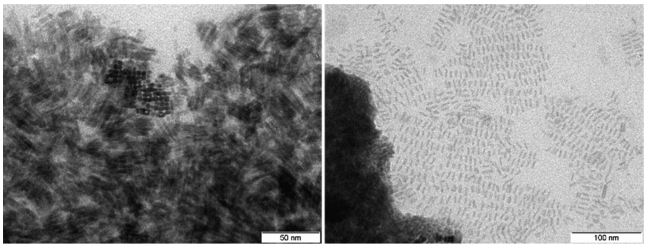

Figure 5. TEM images of the synthetized α-Fe_2O_3 nanorods by a w/o microemulsion method.

adopted synthesis methodology led to the development of monodisperse nanorods 4 nm wide and 11 nm long. The NP morphology may have differed from the spherical particles reported by Chin and Yaacob[39] and Han et al.[40] because of the nature and purity of the surfactant used (hexadecyltrimethylammonium bromide, CTAB).[41]

The ESEM micrographs (Figure S4—Supporting Information) of selected areas (external, inner surface, and cross section) of the original corundum hollow fiber (Φ: 20 nm) presented dissimilar surface topography, which can affect the incorporation of active phases. The cross section displayed a sponge-like symmetric structure. The roughness of the external surface and cross section of the membrane may benefit the distribution and incorporation of the active species.

Compared to the original membrane, the Fe-CMR_i displayed completely different surface features, as can be seen in Figure 6. The impregnated membrane exhibited oxidic aggregates on the external surface (Figure 6A) and, to a lesser extent, on the inner wall (Figure 6C); interestingly, the cross section retained the surface features of the original α-Al_2O_3 membrane (Figure 6B). In line with this, EDX analysis revealed that the Fe species were distributed nonuniformly over the tubular hollow fiber, most of which were incorporated on the external and internal surfaces of the CMR (Figure S5—Supporting Information). The heterogeneous distribution of the impregnated Fe species may result from the high calcination temperature, the vacuum drying stage, and/or the compact structure of corundum.

ESEM−EDX analysis was also performed over Fe-CMR_p and Fe-CMR_m, whose results can be seen in Figures 7 and 8. This analysis corroborated that Fe species were mainly incorporated on the external surface of the hollow fibers.

Similar to the crystallinity of Pd-CMR, Fe-CMR crystallinity was analyzed at various selected areas of the hollow fibers. The μ-XRD analysis of the Fe-CMR_m sample only revealed corundum's characteristic peaks; neither iron oxide phases nor mixed oxides were detected (Figure 9). Nevertheless, the same analysis at different regions of the Fe-CMR_p displayed corundum and incipient hematite peaks (JCPDS 01-071-5088), suggesting the accumulation of oxidic aggregates on the external surface of the membrane (Figure 10). On the one hand, taking into account the low Fe content of the Fe-CMR_p, the presence of hematite peaks might suggest that the preparation methodology did not anchor the Fe species sufficiently in the alumina membrane. Furthermore, this poor Fe anchorage was macroscopically visible, and part of the hematite detached itself from the hollow fiber. On the other hand, the iron incorporation method used for Fe-CMR_m did favor a high dispersion level of the active phase (XRD-silent iron phases).

These results demonstrate that these preparation strategies facilitated different Fe distributions on the CMR as well as surface features that could become useful in other Fe-catalyzed reactions. Moreover, these synthesis strategies may be employed to incorporate other metallic species, thus reducing the content required for active phases, such as precious metals.

2.2.2. Catalytic Results Using the Fe-CMR. Catalytic wet hydrogen peroxide oxidation of phenol involves using a heterogeneous Fenton-like system (Fe solid catalyst with H_2O_2 to produce hydroxyl radicals) for the abatement of refractory pollutants present in wastewater.[43] The phenol oxidation mechanism comprises its decomposition into aromatic compounds, with two hydroxyl groups substituted in the benzene ring (hydroquinone, resorcinol, and catechol). The oxidation of these molecules generates quinone-like compounds (*p*-benzoquinone and *o*-benzoquinone), which can be more toxic than phenol itself. Afterward, further oxidation gives place to the ring opening of aromatic molecules to form carboxylic acids, decreasing the pH of the reaction medium.[44,45]

In this study, we have tested the Fe-CMR prepared using the methodologies presented in this study. The gradual dosage of H_2O_2 can be an advantageous strategy to minimize scavenging

DOI: 10.1021/acsomega.9b02706
ACS Omega 2019, 4, 19818−19828

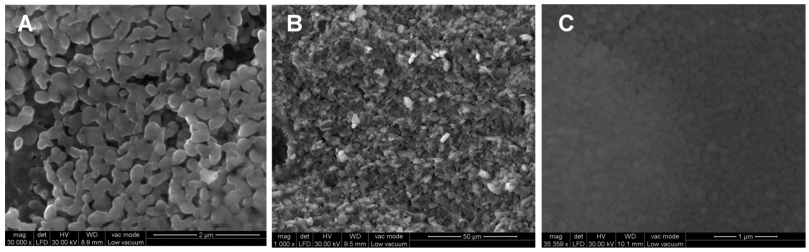

Figure 6. ESEM images for different regions of the impregnated membrane (Fe-CMR_i) and calcined at 900 °C (A: external surface, B: cross section, and C: internal surface).

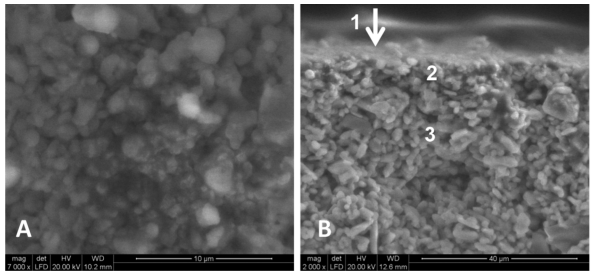

Fe-CMR_p	
Position	Fe content % wt.
1	6
2	5.4
3	0

Figure 7. ESEM–EDX results for different membrane regions of Fe-CMR_p prepared by the precipitation of a Fe complex over the external surface and calcined at 900 °C (A: external surface and B: cross section).

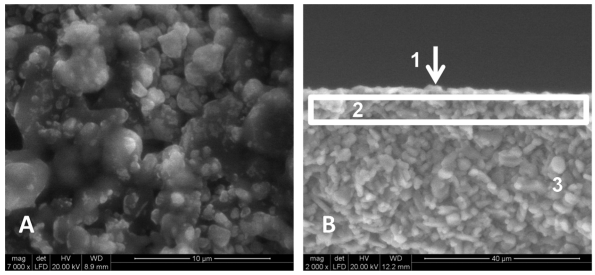

Fe-CMR_m	
Position	Fe content % wt.
1	7
2	0
3	0

Figure 8. ESEM–EDX results for different membrane regions of Fe-CMR_m prepared by reverse filtration of a w/o microemulsion of hematite nanorods and calcined at 900 °C (A: external surface and B: cross section).

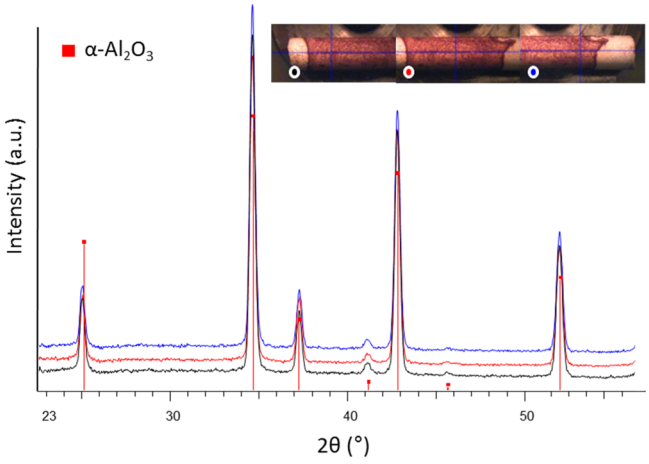

Figure 9. μ-XRD results of the Fe-CMR_m prepared by reverse filtration of a w/o microemulsion of hematite nanorods and calcined at 900 °C.

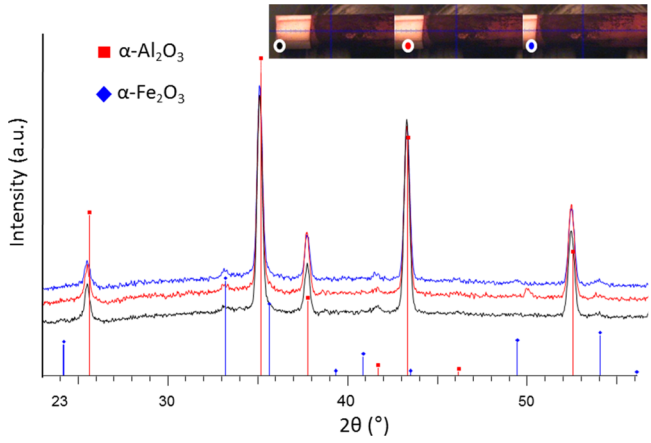

Figure 10. μ-XRD results of the Fe-CMR_p prepared by the precipitation of a Fe complex and calcined at 900 °C.

reactions and enhance its consumption efficiency.[42] According to the contactor–distributor scheme, the oxidant and the organic pollutant make contact on the outer side of the membrane. Consequently, the wet impregnation methodology (Fe-CMR_i) should lead to parasitic decomposition of H_2O_2 inside the hollow fiber because of the direct contact of the oxidant with the active phase in the absence of an organic substrate. In this sense, the availability of Fe on the external surface of the membrane is needed, as for Fe-CMR_p and Fe-CMR_m.

However, our preliminary screening results showed that Fe-CMR_i was the most active reactor, probably because of its

DOI: 10.1021/acsomega.9b02706
ACS Omega 2019, 4, 19818–19828

higher Fe content (entry 5, Table 1). This CMR produced a TOC conversion of ca. 30% (low mineralization level) and 98% phenol removal. Unfortunately, HPLC analysis revealed high selectivity toward the formation of highly toxic dihydroxybenzenes, catechol, and hydroquinone.[43] Additionally, we have observed that the reaction medium pH decreased (around 2) because of the accumulation of carboxylic acids that promoted iron leaching of 7 mg/L (ICP measurements), which is likely to have assisted phenol oxidation. On the other hand, the Fe-CMR_p and Fe-CMR_m reactors did not promote phenol mineralization.

At this point, we can conclude that the Fe-CMRs were better as distributors than as contactor reactors. As the amount of loaded Fe was similar to other studies reported in the literature,[45,46] we consider that its inability to favor H_2O_2 decomposition into hydroxyl radicals (Fenton mechanism) might be related to the inert characteristics of the corundum membrane (absence of acidic sites) and its low surface area of ~3 m^2/g. These observations were in accordance with the results reported by Pestunova et al., who studied the peroxidation of 1 g/L of phenol using Fe-alumina catalysts supported on γ and α-Al_2O_3 at 90 °C. The authors obtained poor phenol mineralization (TOC conversion of 26%) for the catalyst supported on corundum as opposed to the one on γ-Al_2O_3 (TOC conversion of 56%).[47]

3. CONCLUSIONS

CMRs represent an excellent solution to the problems faced when carrying out a three-phase catalytic process. We have successfully managed to develop several methods to produce new CMRs containing one or more catalytic active sites employing the following procedures: impregnation of the active phase, sputtering, reverse filtration of microemulsions, precipitation of a metal complex, or growing the desired material directly into the pores of the CMR.

For the Pd-based CMRs, we have discovered that using the microemulsion procedure leads to small and very well-dispersed Pd NPs by contrast with conventional wet impregnations; therefore, this approach can be useful to minimize the doped Pd concentration and thus the reactor cost. Thinking on advanced industrial processes that might require the presence of several catalysts, we have developed a new method of growing hydrotalcites in the pores of the Pd-CMR.

In the same manner, for the Fe-based CMRs, we have observed that in the case of the impregnation method, the Fe species were distributed nonuniformly over the hollow fiber. On the contrary, by using a Fe nanorod microemulsion and the precipitation of a Fe complex (Prussian blue), the Fe species were incorporated only on the external surface of the CMRs.

To prove the importance of developing these new CMRs, we have studied their activity in two reactions: in situ epoxidation of *trans*-chalcone and peroxidation of phenol.

The hybrid Pd-CMR containing hydrotalcite was able to catalyze two reactions simultaneously: hydrogenation and epoxidation reaction of the α,β-unsaturated ketone. Although the epoxide could not be isolated in all the experiments, the presence of the *cis*-chalcone demonstrates that the reaction setup is active. This entire systematic process is the first one of its kind and illustrates that hydrotalcites incorporated in CMRs open new routes for developing and designing a new type of hybrid reactors.

Regarding the abatement of organic pollutants present in aqueous effluents (peroxidation of phenol), we have observed that to avoid parasitic reactions with the hydrogen peroxide, the active Fe species should be deposited on the external side of the CMR. Nevertheless, the inert nature of the corundum membrane did not contribute toward the effective mineralization of phenol.

Therefore, different preparation procedures can be employed to produce CMRs with unique catalytic activities. Future studies will be carried out to understand and use the full catalytic potential of these new CMRs.

4. EXPERIMENTAL SECTION

4.1. CMR Preparation. Corundum hollow fiber membranes of 1400 and 20 nm filtration pore size (Φ) for ultra- and nanofiltration manufactured by CEPAration were used as the starting materials for the preparation of different palladium- and iron-based CMRs. All the hollow fibers are made of corundum (α-Al_2O_3). The hollow fiber membranes present chemical resistances to different chemicals in a wide range of pH (1−14). Additionally, these fibers have high thermal stability, and as a result, they may be used at temperatures up to 1000 °C. The porosity of the membranes varied from 10 to 15%. The tubular membranes have an inner diameter of 2 mm and an outer diameter of 3 mm with a total length of 300 mm.

4.1.1. Palladium-Based CMR (Pd-CMR). 4.1.1.1. Pd-CMR Obtained by the Sputtering Method. The CMR was prepared using a method already reported in the literature;[15] briefly, palladium was pulverized from a palladium target (Hauner metallische werkstoffe, 99.95% purity) in a standard sputtering chamber and deposited on the external surface of the CMR of 1400 nm porous size using a K575X sputter coater (Quorum Technologies) at 30 mA for 60 s of exposition using pure argon as a working gas. To obtain a homogenous distribution of the noble metal on the CMR using this method, an assembly was used to rotate with 90 rpm (rotation per minute) the hollow fiber membrane, while palladium was pulverized and deposited. A glass plate was placed at the same height with the membrane as a reference material to determine the thickness (amount) of the Pd layer by means of X-ray reflectometry using a Bruker-AXS D8-Discover diffractometer. The thickness of the layer was obtained by X-ray refractometry.

The CMR was dried at 120 °C for 2 h, calcined at 400 °C overnight, and reduced at 350 °C under 20 mL/min of H_2 for 2 h. The amount of palladium deposited onto the membrane was obtained by taking into consideration the thickness of the Pd layer on the glass plate, the effective membrane area exposed to the palladium beam, and the rotation velocity.

This CMR was denoted as Pd-CMR_s. It is worth mentioning that all the Pd_CMRs have the same appearance after reduction, thus Figure 11 presents an example of a CMR before (a) and after the reduction step (b).

4.1.1.2. CMR with PdCu NPs Alloy Loaded by Inverse Impregnation. The microemulsion containing the PdCu precursor was synthesized following a variation of the procedure described in the literature.[48,49] The NPs were

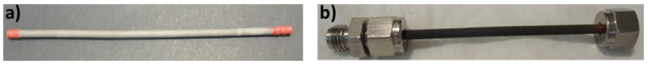

Figure 11. Example of a Pd_CMR before (a) and after the reduction step (b).

DOI: 10.1021/acsomega.9b02706
ACS Omega 2019, 4, 19818−19828

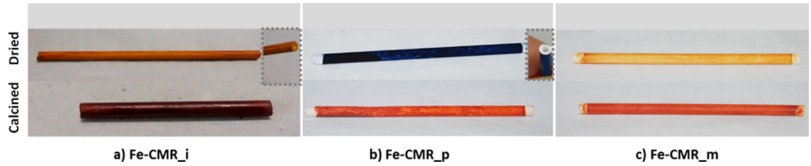

Figure 12. Fe-based CMR prepared by the (a) impregnation method, (b) precipitation of a Fe complex, and (c) reverse filtration of a w/o microemulsion containing hematite NPs.

obtained by mixing two microemulsions of water in oil. Both microemulsions contained 17.78% w/w of CTAB as a surfactant (purity ≥ 96%, Fluka Analytical), 22.22% w/w of *n*-butanol as a cosurfactant (purity 99.8%, Sigma-Aldrich), 40% w/w of *iso*-octane (Pareac), and 20% w/w of an aqueous solution of the metal precursors (PdCu aqueous solution) or reducing agent (0.5 M of hydrazine solution). The PdCu aqueous solution was a mixture of individual precursor solutions to obtain a metal proportion of 80% of Pd and 20% of Cu. The solution of 0.01 M $Pd(NH_3)_4Cl_2$ was prepared by dissolving $PdCl_2$ (Johnson Matthey, 59.83% metal content) in 0.5 N hydrochloric acid; the solution was adjusted to pH 9 using ammonium hydroxide (Sigma-Aldrich). Solution (0.01 M) of $[Cu(NH_3)_4]Cl_2$ was obtained using the similar procedure starting with $CuCl_2$ (Sigma-Aldrich, assay 90). The solution of 0.5 M H_4N_2 was obtained by dissolving H_4N_2OH (hydrazine monohydrate with approximately 64% of hydrazine, Sigma-Aldrich) in Milli-Q water. The two microemulsions were vigorously stirred at ambient temperature. In order to produce the palladium−copper NPs, both microemulsions were mixed and rapidly stirred at 450 rpm. To eliminate the excess surfactant, the solution was washed with ethanol and centrifuged. The PdCu NP deposition onto the external surface of the chosen membrane was performed by a simple filtration procedure from the outside to the inside of the membrane. The PdCu NPs suspended in ethanol were placed in a 100 mL test tube, and the solution was continuously stirred. The hollow fiber membrane of 1400 nm pore size was placed in the test tube. One end of the CMR was tightly closed, and the other end was connected to vacuum. A cold trap was coupled to the vacuum line to recover the permeated ethanol. The level of liquid in the tube was maintained by continuously adding fresh ethanol. During the filtration, the PdCu NPs were retained on the external membrane surface in a homogeneous manner because of the continuous stirring process. In order to measure the amount of palladium loaded onto the membrane, a mass balance was realized from measurements by ICP. For this analysis, samples from the different solutions were collected: the initial and final feed solution from the test tube containing the suspended PdCu NPs and the permeate solution retained in the cold trap.

The CMR was dried in a special vessel under vacuum for 30 min. Furthermore, the CMR was dried at 120 °C for 2 h, calcined at 550 °C for 6 h, and reduced under a hydrogen flow (20 mL/min) at 350 °C for 3 h.

The resulting catalytic reactor was denoted as PdCu-CMR_m.

4.1.1.3. Pd-CMR and Mg−Al Hydrotalcite by the Impregnation Method. The palladium impregnation technique was already explained elsewhere.[15,18] The impregnation of the CMR with Pd was done as follows: a known amount of the precursor salt solution of palladium ($PdCl_2$ from Johnson Matthey, 59.83% noble metal) was added into Milli-Q water under stirring, over which concentrated hydrochloric acid (purity grade of 37%, Sigma-Aldrich) was added dropwise until the salt was completely dissolved. Finally, the concentration was adjusted with Milli-Q water in order to achieve approximately 1% of weight of Pd per weight of the membrane. The palladium precursor solution was impregnated into the membrane of 1400 nm of pore size. Once the impregnation was complete, the CMR was dried in a special vessel under vacuum for 30 min. In this step, the CMR was rotated along the horizontal axis in order to avoid preferential deposition of the salts onto the ceramic support. Furthermore, the CMR was dried at 120 °C for 5 h, calcined at 450 °C overnight, and reduced under 20 mL/min of hydrogen at 350 °C for 3 h. The amount of palladium deposited was calculated by the weight difference between the original and the modified membrane. The final CMR was divided into two equal parts of 15 cm. For the preparation of the hybrid reactors, two procedures were used:

Method A: Mg−Al HT was prepared separately and then loaded on the CMR. The HT containing Mg−Al ratio 2:1 was prepared by the coprecipitation method at room temperature and pH = 10. The appropriate amounts of $Mg(NO_3)_2{\cdot}6H_2O$ and $Al(NO_3)_3{\cdot}9H_2O$ (Sigma-Aldrich) were dissolved in 110 mL of Milli-Q water and added dropwise into a vessel containing 150 mL of Milli-Q water. The pH was kept constant using 2 M NaOH solution. The suspension was stirred overnight at room temperature. The obtained solid was filtered and washed several times with Milli-Q water and dried under vacuum. The Pd-CMR (prepared by impregnation, having a length of 15 cm and a nominal pore size of 1400 nm) with one end closed was attached to a vacuum system and introduced into a recipient containing Mg−Al HT suspended in solution (containing 2 wt % HT with respect to the CMR). The entire system was continuously stirred. Under vacuum, the HT was retained on the external surface of the CMR. This process was repeated three times, and then the CMR was washed with MilliQ water several times, dried, and calcined at 450 °C in air overnight. Finally, the hybrid CMR was reduced under 15 mL/min of H_2 for 3 h at room temperature. The CMR was denoted as HT-Pd-CMR_i_a.

Method B: The Pd-CMR with both ends closed was introduced first into a solution containing $Mg(NO_3)_2{\cdot}6H_2O$ and left there for 3 min, then introduced into a solution of $Al(NO_3)_3{\cdot}9H_2O$, and left there for 3 min. This process was repeated three times to assure a 2 wt % HT deposited on the CMR (prepared by impregnation, having a length of 15 cm and a nominal pore size of 1400 nm), and afterward, without washing, the CMR was introduced into a 2 M NaOH solution and left there for 10 min. After this, the CMR was washed with MilliQ water overnight, dried, and calcined at 450 °C in air overnight. Finally, the hybrid CMR was reduced for 2 h at room temperature under H_2 flow. The CMR was denoted as HT-Pd-CMR_i_b.

4.1.2. Iron-Based CMR (Fe-CMR). 4.1.2.1. Iron-Based CMR by the Impregnation Method. The tubular hollow fiber (Φ

DOI: 10.1021/acsomega.9b02706
ACS Omega 2019, 4, 19818−19828

(nominal pore size): 20 nm; length: 75 mm) was impregnated with a Fe precursor solution using an incipient wetness technique. The membrane was submerged in a highly concentrated solution of ferric chloride ($FeCl_3 \cdot 6H_2O$ Sigma-Aldrich, 97%). The precursor solution was forced to penetrate the entire surface of the membrane repeatedly. Thereafter, the impregnated membrane was dried in several stages so as to promote a homogeneous distribution of the active phase. First, the excess liquid was removed by drying the CMR under vacuum for 15 min. Next, the hollow fiber was dried overnight at room temperature before being heated in an oven at 110 °C for 24 h (static air atmosphere). Finally, the impregnated membrane was calcined in a muffle furnace at 900 °C for 4 h (10 °C/min, static air atmosphere). This CMR, whose visual aspect is depicted in Figure 12a, was given the name Fe-CMR_i. Its final Fe content was determined by the weight difference between the fresh membrane and the calcined CMR.

4.1.2.2. Precipitation of a Fe Complex on the External Surface of the Membrane. To ensure that the Fe species were deposited on the external surface of the tubular hollow fiber, a Fe complex (Prussian blue $Fe_3[Fe(CN)_6]_2$) was precipitated on the external part of the membrane by separating the Fe precursor salts from the reducing agent (hydrogen peroxide). For this, we used a modified version of the method reported by Doumic et al.[50] Preparation of the Fe complex involved exposing the membrane's exterior to a stirred aqueous solution of ferric chloride (0.1 M) and potassium ferricyanide $K_3[Fe(CN)_6]$ (0.1 M, Sigma-Aldrich, ≥ 99%) for 10 min; at the same time, hydrogen peroxide (30 wt %) was continuously supplied from inside the membrane at a flow rate of 2 mL/h. The proper adjustment of the contact time and the flow of H_2O_2 were key to achieving a good adhesion of the complex on the membrane's outer surface. For homogeneous distribution of the active phase, the membrane (Φ: 20 nm; length: 75 mm) was positioned vertically inside a 100 mL test tube and operated as a semicontinuous contactor−distributor system. This scheme was based on a communicating vessel arrangement between the reservoir containing the H_2O_2 feeding solution and the test tube with the Fe precursor's solution. This configuration kept the pressure balanced, thus keeping constant the permeate flow of the reducing agent. The hydrogen peroxide was supplied by means of a peristaltic pump, forcing its recirculation into the feeding tank, favoring the elimination of bubbles accumulated in the inner zone of the membrane. The experimental setup was depicted in Figure S6.

Afterward, the membranes were dried and calcined at 900 °C, as explained above (see Section 4.1.2.1). This CMR was named Fe-CMR_p, and Figure 12b displays its visual appearance.

4.1.2.3. CMR with α-Fe_2O_3 Nanorods Loaded by Reverse Filtration of a w/o Microemulsion. Another strategy was to prepare a microemulsion of hematite NPs and incorporate them into the hollow fiber by an inverse filtration procedure. Hematite NPs were synthesized by the water-in-oil microemulsion method adapting different experimental protocols already reported in the literature.[30,31] The iron oxide NPs were obtained by mixing two w/o microemulsions. Hexadecyl trimethyl ammonium bromide (Fluka, ≥ 96%), *n*-butanol (Sigma-Aldrich, 99.8%), *n*-octane (Sigma-Aldrich, ≥ 99%), ferric chloride (Sigma-Aldrich), sodium hydroxide, and ultrapure water (Milli-Q water, Millipore) were used as the surfactant, cosurfactant, oil phase, Fe precursor, precipitant agent, and aqueous phase, respectively. Both microemulsions were prepared by adjusting the surfactant, cosurfactant, and oil phase at a molar ratio of 1:3.9:9. The microemulsion containing the Fe species aqueous solution was a mixture of ferric chloride (0.4 M) and trace amounts of ferrous chloride (Sigma-Aldrich) by using molar ratios of Fe(II)/Fe(III) = 0.08 and water/surfactant = 10.9. Similarly, a second microemulsion containing aqueous solution of NaOH (0.25 M) was prepared. The two microemulsions were stirred at room temperature until they became transparent. Afterward, the NaOH microemulsion was added dropwise to the stirred microemulsion containing the Fe species using a volumetric ratio of 1:1. After mixing, the solution turned reddish−brown, indicating the formation of the precipitate. The final microemulsion was heated at 105 °C and refluxed for 24 h under vigorous stirring.

These NPs were incorporated into the external surface of the membrane (Φ: 20 nm; length: 75 mm) by using an analogous reverse filtration procedure as reported in Section 4.1.1.2. Likewise, the final Fe content deposited on the membrane was determined using ICP, as described earlier in Section 4.1.1.2. The membranes were dried and calcined at 900 °C (see Section 4.1.2.1). The CMR was labeled as Fe-CMR_m, and Figure 12c shows its visual aspect.

4.2. Catalytic Testing. *4.2.1. In Situ Epoxidation of trans-Chalcone.* One end of the CMR was tightly closed, and to the other end, a flow of H_2 was supplied by means of a mass flow controller (30 mL/min). The CMR was immersed in a reaction vessel, which contained 40 mL of solvent and 10 mg of *trans*-chalcone. In order to test the influence of solvents upon the outcome of the reaction, different polar aprotic, polar protic, and nonpolar solvents were used: water, ethanol, methanol, acetonitrile propanol, dimethyl sulfoxide, and heptane. The reaction was performed at room temperature and normal pressure, and after 6 h, the solvent was removed by vacuum distillation and the products were analyzed by ^{1}H NMR. Selectivity was computed from ^{1}H NMR spectra.

4.2.2. Peroxidation of Phenol. The operating conditions consisted of $[phenol]_0$ = 5 g/L, stoichiometric dosage of hydrogen peroxide ($[H_2O_2]_0$ = 0.75 mol/L), T = 70 °C and atmospheric pressure, reaction time = 4 h, and pH_0 = 3. Figure S6 in the Supporting Information shows the semicontinuous reaction system implemented; this scheme consisted in an experimental setup similar to that applied in the preparation of Fe-CMR_p (see Section 4.1.2.2). In this case, the oxidant agent (hydrogen peroxide) was gradually supplied at a rate of 2 mL/h (30 wt %) from the inner side and put in contact with the phenolic solution at the external surface of the CMR. Catalytic performance was monitored in terms of phenol concentration (HPLC) and TOC removal. Liquid samples were taken at different time intervals and analyzed, as reported elsewhere.[28,46]

■ ASSOCIATED CONTENT

Supporting Information

The Supporting Information is available free of charge on the ACS Publications website at DOI: 10.1021/acsomega.9b02706.

Detailed characterization techniques for materials and reaction products; pictorial presentation of the reaction setup of the Fe-based CMRs under semicontinuous operation; XRD of the membrane; ^{1}H NMR spectra of

DOI: 10.1021/acsomega.9b02706
ACS Omega 2019, 4, 19818−19828

reaction products; and detailed ESEM and EDX images of the Fe-based CMR (PDF)

AUTHOR INFORMATION

Corresponding Author

*E-mail: anton.dafinov@urv.cat. Phone: +34 977558112. Fax: +34977559621.

ORCID

Verónica Pinos-Vélez: 0000-0001-8278-5873

Author Contributions

V.P.-V., C.d.L., D.G.C., and A.D. conceived and designed the experiments; V.P.-V., C.d.L., D.G.C., and A.D. interpreted the data and wrote the paper; V.P.-V., C.d.L., D.G.C., F.M., and A.D. read, corrected, and approved the final version of manuscript

Notes

The authors declare no competing financial interest.

ACKNOWLEDGMENTS

V.P.-V. expresses her gratitude for the economic support given by SENESCYT and Universidad de Cuenca. D.G.C. is grateful to the Spanish Government's MECD for the FPU predoctoral grant. C.d.L. thanks CONICET, UNMdP, ANPCyT, and Programa BECAR (Argentina) for financial support.

REFERENCES

(1) Mo, Y.; Imbrogno, J.; Zhang, H.; Jensen, K. F. Scalable thin-layer membrane reactor for heterogeneous and homogeneous catalytic gas−liquid reactions. *Green Chem.* **2018**, *20*, 3867−3874.

(2) Biardi, G.; Baldi, G. Three-Phase Catalytic Reactors. *Catal. Today* **1999**, *52*, 223−234.

(3) Yamada, Y. M. A.; Watanabe, T.; Torii, K.; Uozumi, Y. Catalytic Membrane-Installed Microchannel Reactors for One-Second Allylic Arylation. *Chem. Commun.* **2009**, 5594−5596.

(4) Zhang, G.; Jin, W.; Xu, N. Design and Fabrication of Ceramic Catalytic Membrane Reactors for Green Chemical Engineering Applications. *Engineering* **2018**, *4*, 848−860.

(5) Shu, J.; Grandjean, B. P. A.; Neste, A. V.; Kaliaguine, S. Catalytic Palladium-Based Membrane Reactors: A Review. *Can. J. Chem. Eng.* **1991**, *69*, 1036−1060.

(6) Saracco, G.; Specchia, V. Catalytic Inorganic-Membrane Reactors: Present Experience and Future Opportunities. *Catal. Rev.: Sci. Eng.* **1994**, *36*, 305−384.

(7) Centi, G.; Dittmeyer, R.; Perathoner, S.; Reif, M. Tubular Inorganic Catalytic Membrane Reactors: Advantages and Performance in Multiphase Hydrogenation Reactions. *Catal. Today* **2003**, *79−80*, 139−149.

(8) Miachon, S.; Dalmon, J.-A. Catalysis in Membrane Reactors: What About the Catalyst? *Top. Catal.* **2004**, *29*, 59−65.

(9) Kumari, P.; Bahadur, N.; Dumée, L. F. Photo-Catalytic Membrane Reactors for the Remediation of Persistent Organic Pollutants − A Review. *Sep. Purif. Technol.* **2019**, *230*, 115878.

(10) Seidel-Morgenstern, A. *Membrane Reactors: Distributing Reactants to Improve Selectivity and Yield*; Wiley-VCH, 2010; pp 1−13.

(11) Abdallah, H. Review on Catalytic Membranes Production and Applications. *Bull. Chem. React. Eng. Catal.* **2017**, *12*, 136−156.

(12) Abate, S.; Centi, G.; Melada, S.; Perathoner, S.; Pinna, F.; Strukul, G. Preparation, Performances and Reaction Mechanism for the Synthesis of H_2O_2 From H_2 and O_2 Based on Palladium Membranes. *Catal. Today* **2005**, *104*, 323−328.

(13) Melada, S.; Pinna, F.; Strukul, G.; Perathoner, S.; Centi, G. Palladium-Modified Catalytic Membranes for the Direct Synthesis of H_2O_2: Preparation and Performance in Aqueous Solution. *J. Catal.* **2005**, *235*, 241−248.

(14) Pashkova, A.; Svajda, K.; Dittmeyer, R. Direct Synthesis of Hydrogen Peroxide in a Catalytic Membrane Contactor. *Chem. Eng. J.* **2008**, *139*, 165−171.

(15) Osegueda, O.; Dafinov, A.; Llorca, J.; Medina, F.; Suerias, J. In situ generation of hydrogen peroxide in catalytic membrane reactors. *Catal. Today* **2012**, *193*, 128−136.

(16) Liu, C.; Xu, Y.; Liao, S.; Yu, D.; Zhao, Y.; Fan, Y. Selective Hydrogenation of Propadiene and Propyne in Propene with Catalytic Polymeric Hollow-Fiber Reactor. *J. Membr. Sci.* **1997**, *137*, 139−144.

(17) Urbanczyk, D.; Dittmeyer, R.; Wolf, A.; Warsitz, R.; Fischer, G.; Voigt, I. Evaluation of Porous Catalytic Membranes Operated in Pore-Flow-Through Mode for Hydrogenation of α-Methylstyrene. *Asia-Pac. J. Chem. Eng.* **2010**, *5*, 12−25.

(18) Pinos, V. P.; Crivoi, D. G.; Medina, F.; Sueiras, J. E.; Dafinov, A. I. New Tuneable Catalytic Membrane Reactor for Various Reactions in Aqueous Media. *ChemistrySelect* **2016**, *1*, 124−126.

(19) Pinos, V.; Dafinov, A.; Medina, F.; Sueiras, J. Chromium(VI) Reduction in Aqueous Medium by Means of Catalytic Membrane Reactors. *J. Environ. Chem. Eng.* **2016**, *4*, 1880−1889.

(20) Pinos-Vélez, V.; Medina, F.; Dafinov, A. Performance of the Catalytic Membrane Reactors of Different Pore Size with Palladium as Catalytic Phase in Hydrogenation and Oxidation Reactions. *Braz. J. Chem. Eng.* **2018**, *35*, 1257−1266.

(21) di Luca, C.; Massa, P.; Fenoglio, R.; Cabello, F. M. Improved Fe_2O_3/Al_2O_3 as Heterogeneous Fenton Catalysts for the Oxidation of Phenol Solutions in a Continuous Reactor. *J. Chem. Technol. Biotechnol.* **2014**, *89*, 1121−1128.

(22) di Luca, C.; Ivorra, F.; Massa, P.; Fenoglio, R.; Cabello, F. M. Improved Fe_2O_3/Al_2O_3 Systems for the Oxidation of a Model Organic Pollutant Using H2O2 as Oxidant. *Curr. Catal.* **2014**, *3*, 161−165.

(23) Mengers, H.; Benes, N. E.; Nijmeijer, K. Multi-Component Mass Transfer Behavior in Catalytic Membrane Reactors. *Chem. Eng. Sci.* **2014**, *117*, 45−54.

(24) Iulianelli, A.; Basile, A. Advances on Inorganic Membrane Reactors for Production of Hydrogen. *Fuel Cells and Hydrogen Production*; Springer: New York, NY, 2019; pp 935−945.

(25) Enthaler, S.; Junge, K.; Beller, M. Sustainable Metal Catalysis with Iron: From Rust to a Rising Star. *Angew. Chem.* **2008**, *47*, 3317−3321.

(26) Leal, T. W.; Lourenço, L. A.; Brandão, H. d. L.; da Silva, A.; de Souza, S. M. A. G. U.; de Souza, A. A. U. Low-cost iron-doped catalyst for phenol degradation by heterogeneous Fenton. *J. Hazard. Mater.* **2018**, *359*, 96−103.

(27) Crivoi, D.-G.; Segarra, A. M.; Medina, F. Highly selective multifunctional nanohybrid catalysts for the one-pot synthesis of α,β-epoxy-chalcones. *J. Catal.* **2016**, *334*, 120−128.

(28) Osegueda, O.; Dafinov, A.; Llorca, J.; Medina, F.; Sueiras, J. Heterogeneous Catalytic Oxidation of Phenol by In-Situ Generated Hydrogen Peroxide Applying Novel Catalytic Membrane Reactors. *Chem. Eng. J. (Amsterdam, Neth.)* **2015**, *262*, 344−355.

(29) Marcano, J. G. S.; Tsotsis, T. T. *Catalytic Membranes and Membrane Reactors*; Wiley-VCH, 2002.

(30) Vospernik, M.; Pintar, A.; Levec, J. Application of a Catalytic Membrane Reactor to Catalytic Wet Air Oxidation of Formic Acid. *Chem. Eng. Process.* **2006**, *45*, 404−414.

(31) Shi, L.; Goldbach, A.; Zeng, G.; Xu, H. H2O2 Synthesis Over PdAu Membranes. *Catal. Today* **2010**, *156*, 118−123.

(32) Pashkova, A.; Dittmeyer, R.; Kaltenborn, N.; Richter, H. Experimental Study of Porous Tubular Catalytic Membranes for Direct Synthesis of Hydrogen Peroxide. *Chem. Eng. J.* **2010**, *165*, 924−933.

(33) Alame, M.; Abusaloua, A.; Pera-Titus, M.; Guilhaume, N.; Fiaty, K.; Giroir-Fendler, A. High-Performance Catalytic Wet Air Oxidation (CWAO) of Organic Acids and Phenol in Interfacial Catalytic Membrane Contactors Under Optimized Wetting Conditions. *Catal. Today* **2010**, *157*, 327−333.

DOI: 10.1021/acsomega.9b02706
ACS Omega 2019, 4, 19818−19828

(34) Shi, L.; Goldbach, A.; Zeng, G.; Xu, H. Direct H2O2 Synthesis Over Pd Membranes at Elevated Temperatures. *J. Membr. Sci.* **2010**, *348*, 160−166.
(35) Inoue, T.; Tanaka, Y.; Pacheco Tanaka, D. A.; Suzuki, T. M.; Sato, K.; Nishioka, M.; Hamakawa, S.; Mizukami, F. Direct Production of Hydrogen Peroxide from Oxygen and Hydrogen Applying Membrane-Permeation Mechanism. *Chem. Eng. Sci.* **2010**, *65*, 436−440.
(36) Cativiela, C.; Figueras, F.; Fraile, J.; García, J.; Mayoral, J. Hydrotalcite-promoted epoxidation of electron-deficient alkenes with hydrogen peroxide. *Tetrahedron Lett.* **1995**, *36*, 4125−4128.
(37) Climent, M. J.; Corma, A.; Iborra, S.; Velty, A. Designing the adequate base solid catalyst with Lewis or Bronsted basic sites or with acid−base pairs. *J. Mol. Catal. A: Chem.* **2002**, *182*−*183*, 327−342.
(38) Kelly, D. R.; Caroff, E.; Flood, R. W.; Heal, W.; Roberts, S. M. The isomerisation of (Z)-3-[^{2}H1]-phenylprop-2-enone as a measure of the rate of hydroperoxide addition in Weitz−Scheffer and Juliá−Colonna epoxidations. *Chem. Commun.* **2004**, 2016−2017.
(39) Chin, A. B.; Yaacob, I. I. Synthesis and Characterization of Magnetic Iron Oxide Nanoparticles via w/o Microemulsion and Massart's Procedure. *J. Mater. Process. Technol.* **2007**, *191*, 235−237.
(40) Han, L.-H.; Liu, H.; Wei, Y. In-Situ Synthesis of Hematite Nanoparticles Using a Low-Temperature Microemulsion Method. *Powder Technol.* **2011**, *207*, 42−46.
(41) Smith, D. K.; Korgel, B. A. The Importance of the CTAB Surfactant on the Colloidal Seed-Mediated Synthesis of Gold Nanorods. *Langmuir* **2008**, *24*, 644−649.
(42) Perathoner, S.; Centi, G. Wet hydrogen peroxide catalytic oxidation (WHPCO) of organic waste in agro-food and industrial streams. *Top. Catal.* **2005**, *33*, 207−224.
(43) Zazo, J. A.; Casas, J. A.; Mohedano, A. F.; Rodriguez, J. J. Semicontinuous Fenton Oxidation of Phenol in Aqueous Solution. A Kinetic Study. *Water Res.* **2009**, *43*, 4063−4069.
(44) Mijangos, F.; Varona, F.; Villota, N. Changes in Solution Color During Phenol Oxidation by Fenton Reagent. *Environ. Sci. Technol.* **2011**, *40*, 5538−5543.
(45) di Luca, C.; Massa, P.; Grau, J. M.; Marchetti, S. G.; Fenoglio, R.; Haure, P. Highly dispersed Fe^{3+}-Al $_2O_3$ for the Fenton-like oxidation of phenol in a continuous up-flow fixed bed reactor. Enhancing catalyst stability through operating conditions. *Appl. Catal., B* **2018**, *237*, 1110−1123.
(46) di Luca, C.; Ivorra, F.; Massa, P.; Fenoglio, R. Iron-Alumina Synergy in the Heterogeneous Fenton-Type Peroxidation of Phenol Solutions. *Chem. Eng. J. (Amsterdam, Neth.)* **2015**, *268*, 280−289.
(47) Pestunova, O. P.; Ogorodnikova, O. L.; Parmon, V. N. Studies on the Phenol Wet Peroxide Oxidation in the Presence of Solid Catalysts. *Chem. Sustain. Dev.* **2003**, *11*, 227−232.
(48) Pinos, V.; Medina, F.; Dafinov, A. Preparation and Characterization of Catalytic Membrane Reactors. *Rev. Fac. Cienc. Quím* **2017**, *16*, 1−14.
(49) Wang, C.-C.; Chen, D.-H.; Huang, T.-C. Synthesis of Palladium Nanoparticles in Water-in-Oil Microemulsions. *Colloid. Surf. Physicochem. Eng. Asp.* **2001**, *189*, 145−154.
(50) Doumic, L.; Salierno, G.; Cassanello, M.; Haure, P.; Ayude, M. Efficient Removal of Orange G Using Prussian Blue Nanoparticles Supported Over Alumina. *Catal. Today* **2015**, *240*, 67−72.

DOI: 10.1021/acsomega.9b02706
ACS Omega 2019, 4, 19818−19828